Structural Engineering and Mechanics, Vol. 17, No. 6 (2004) 879-898
DOI: http://dx.doi.org/10.12989/sem.2004.17.6.879

A continuity method for bridges constructed with precast prestressed concrete girders

Hwan Woo Lee†

Department of Civil Engineering, Pukyong National University, San 100, Yongdangdong, Namgu, Busan 608-739, Korea

Robert W. Barnes‡

Department of Civil Engineering, 238 Harbert Engineering Center, Auburn University, Alabama 36849-5337, U.S.A.

Kwang Yang Kim‡†

Department of Civil Engineering, Pukyong National University, San 100, Yongdangdong, Namgu, Busan 608-739, Korea

(Received August 25, 2003, Accepted March 30, 2004)

Abstract. A method of making simply supported girders continuous is described for bridges with spans of 30-45 m. The splicing method takes advantage of an induced secondary moment to transform the self-weight stresses in the precast simply supported girders into values representative of a continuous girder. The secondary moment results from prestressing of continuity tendons and detensioning of temporary tendons in the girders. Preliminary sections are selected for spliced U-girder bridges with a range of span lengths. Use of the proposed technique results in girder depth reductions of 500-800 mm when compared to standard simply supported I-girder bridges. The flexural behavior of an example bridge with 40-m spans is examined to illustrate the necessary considerations for determining the optimum sequence of splicing operations.

Key words: bridge; continuity method; prestressed concrete; secondary moment; staged prestressing; structural efficiency; U-girder.

1. Introduction

I-shaped simply supported precast prestressed concrete girders are frequently used for short-to-medium span bridges. However, it has been recognized in practice that the required depth of this type of cross section rapidly increases as the span length exceeds approximately 30 m. Therefore,

† Associate Professor
‡ Assistant Professor
‡† Graduate Student

the economic and aesthetic effectiveness of the I-shaped section is limited for longer spans. For this reason, simply supported I-shaped girders are rarely used for spans longer than 30 m in Korea (Korea Highway Corporation 1996). In the United States of America for example, Ralls *et al.* (1993) state that the limits of the cost-effective span lengths in Texas are 37 m and 27 m for the most common I-section depths of 1.37 m and 1.02 m, respectively.

There have been other investigations of methods for increasing the structural efficiency of moderate-span bridges. These can be divided into two general categories. The first category focuses on improving the sectional efficiency of girders or exploiting higher material strengths. Ralls *et al.* (1993) have introduced a U-shaped precast girder as an economic and aesthetic alternative to two I-shaped girders. Simply supported prestressed girders fabricated with high strength concrete have also been studied (Russell 1994, Weigel *et al.* 2003).

The second category of investigations focuses on developing girder-splicing methods to improve structural efficiency (Tadros *et al.* 1993, Ronald 2001, Girgis *et al.* 2002). Tadros *et al.* (1993) have proposed a technique in which prestressing strands in the upper flange of I-sections are spliced to provide continuity. The completed structure becomes a statically indeterminate system. Total stresses in the girders result from a combination of (1) stresses induced by the self-weight of the precast girder in a simply supported state before splicing and (2) stresses resulting from superimposed dead loads and traffic loads applied to the indeterminate structural system after splicing.

A new splicing method for two simply supported girders has been conceived to optimize the beam depth in bridges with spans of 30-45 m while taking advantage of the ease of construction characteristic of simply supported precast girder bridges (Lee *et al.* 2000). This paper introduces the mechanical characteristics of the proposed splicing technique. The structural efficiency of preliminarily designed sections is estimated by comparison with existing sections. Additionally, the flexural behavior of an example bridge is described to illustrate the control of prestressing forces during the splicing stage of the construction procedure.

2. Proposed splicing method

2.1 Construction procedure

Fig. 1 is a conceptual diagram of the construction procedure for the proposed splicing technique. The primary girders are precast and post-tensioned because they can be fabricated with a higher quality material and easily installed on site. Thus, the proposed technique benefits from plant production efficiencies inherent to simply supported girder bridges.

Figs. 1(a) and (e) depict tensioning of permanent beam tendons, tensioning of temporary beam tendons, detensioning of temporary beam tendons, and tensioning of continuity tendons. The partial post-tensioning and detensioning processes that occur in the joint region between the two spans induce an intentional secondary moment, which is further explained in the following section. This induced secondary moment can transform the stress distribution due to self-weight in the simply supported girders into a stress distribution similar to that which would have resulted if the two spans had been originally constructed as a continuous beam. Hence, the spliced spans are able to resist both self-weight and live loads as a continuous structure despite being originally constructed of two simply supported girders.

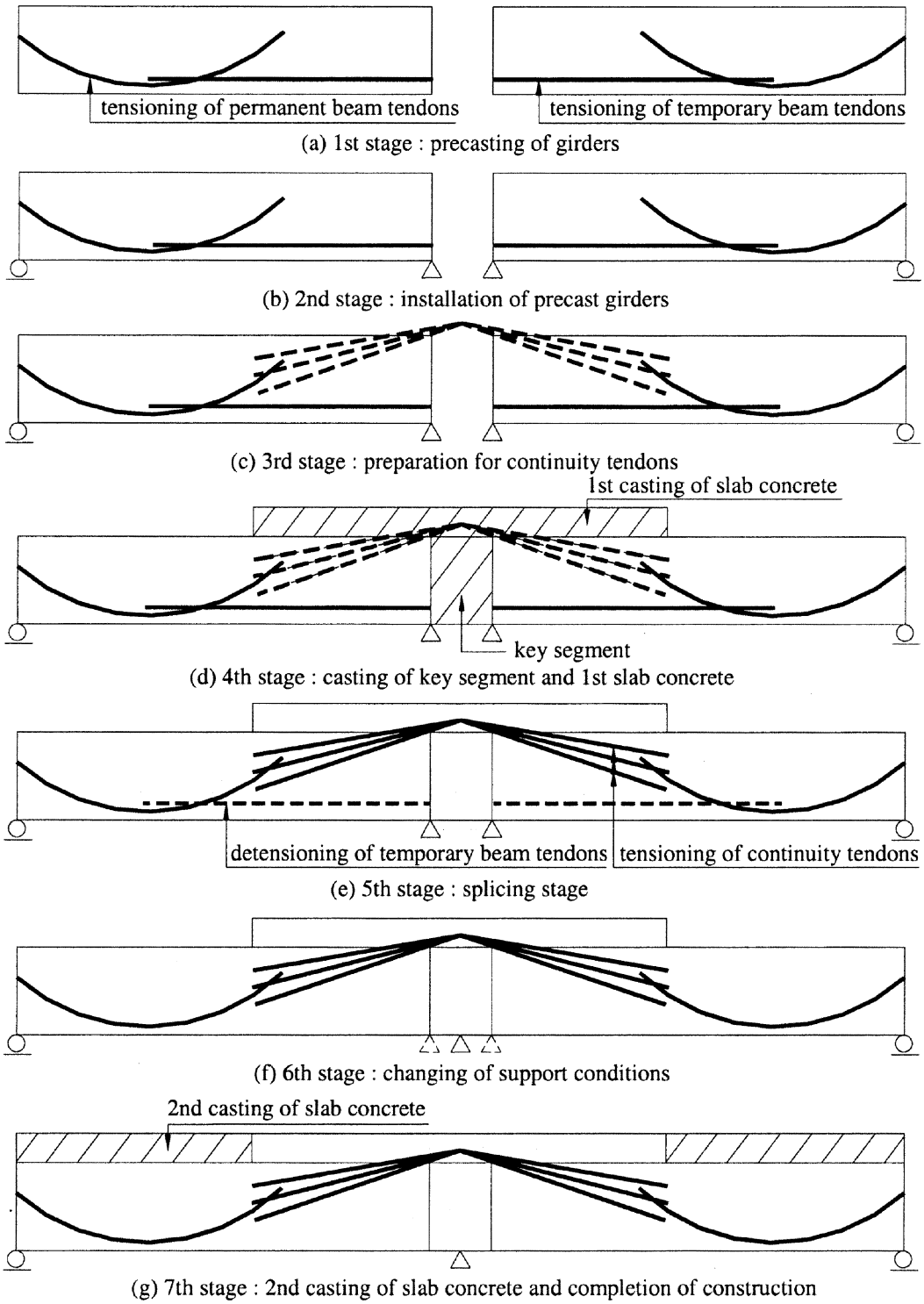

(a) 1st stage : precasting of girders

(b) 2nd stage : installation of precast girders

(c) 3rd stage : preparation for continuity tendons

(d) 4th stage : casting of key segment and 1st slab concrete

(e) 5th stage : splicing stage

(f) 6th stage : changing of support conditions

(g) 7th stage : 2nd casting of slab concrete and completion of construction

Fig. 1 Splicing process for two simply supported U-shaped prestressed girders

2.2 Induced secondary moment

When two precast members are installed as shown in Fig. 1(b), positive bending moments due to self-weight will occur in both simply supported spans as shown in Fig. 2(a). These positive bending moments result in a downward deflection of each span.

Tensioning of continuity tendons at the splicing stage, shown in Fig. 1(e), causes a primary positive bending moment in the sections near the continuous support. Detensioning of the temporary beam tendons, which are already tensioned at the time shown in Fig. 1(a), is performed

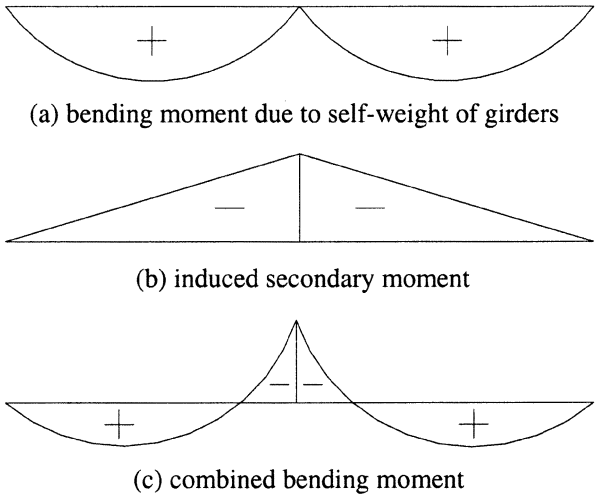

Fig. 2 Conceptual bending moment diagrams during splicing process

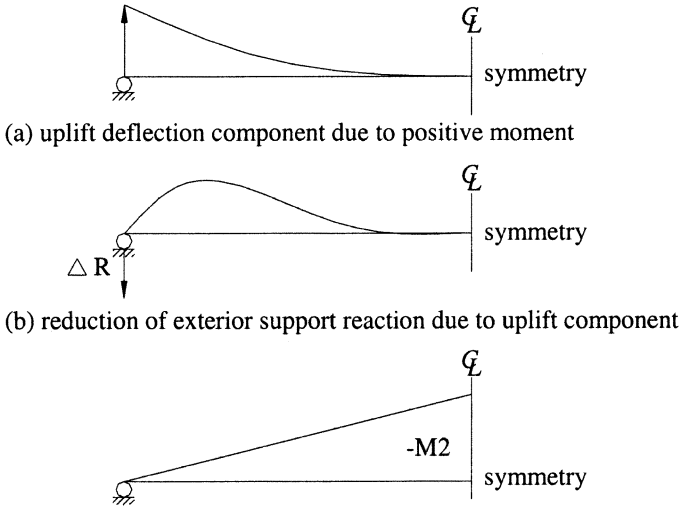

Fig. 3 Generation of secondary moment during splicing process

simultaneously with the tensioning of continuity tendons as shown in Fig. 1(e). The bending moment produced by the original tensioning of the temporary beam tendons is negative. Therefore, detensioning the temporary beam tendons corresponds to introducing a primary positive bending moment in this region.

These positive bending moments induced near the joint region of the spliced girders cause an uplift deflection in each span as shown in Fig. 3(a). However, the girder self-weight deflection component overcomes this uplift component, and a reduction in the reaction force at each exterior supports results. As indicated in Fig. 3(b), this reduction is equivalent to the downward force required to overcome the uplift deflection component at the support. The resulting change in reaction forces causes the development of a secondary moment in the spliced girders as shown in Fig. 3(c).

Finally, superposition of the secondary moment of Fig. 2(b), induced during the splicing stage, transforms the simply supported girder stress distribution into the continuous girder stress distribution shown in Fig. 2(c).

3. Preliminary design and assessment of structural efficiency

3.1 General design conditions

In order to estimate its relative structural efficiency, the proposed splicing method was applied to the design of several bridges with spans of 25 m, 30 m, 35 m, 40 m, and 45 m.

A U-shaped section was adopted for the girders. To match existing I-girder bridges, it was

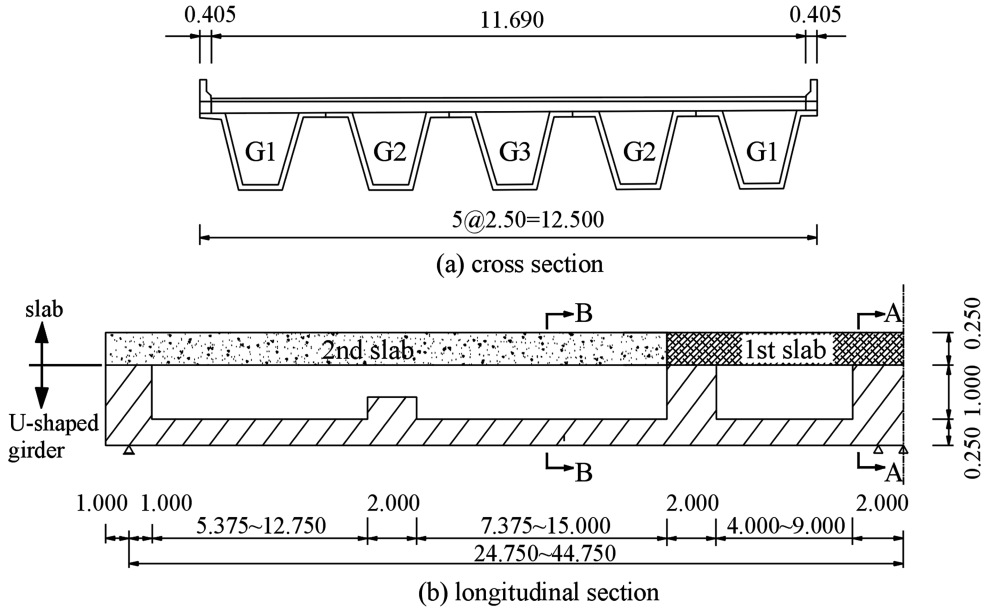

Fig. 4 General sections (unit: m)

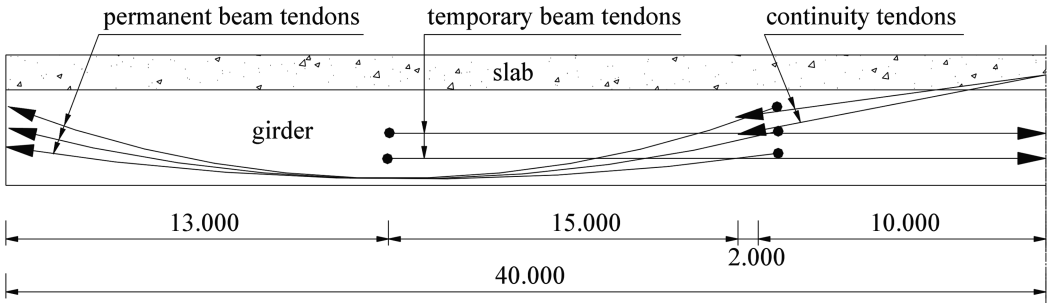

Fig. 5 Conceptual tendon layouts (unit: m)

Table 1 Material properties

Description		Material property
Concrete	U-shaped girder	$f_c' = f_{ci}' = 39.2$ MPa
	1st slab	$f_c' = f_{ci}' = 26.5$ MPa
	2nd slab	$f_c' = 26.5$ MPa
Tendons	Permanent beam tendons	ϕ12.7 mm × 13 strands per duct $f_{pi} = 0.8 f_{py} = 1{,}255.3$ MPa
	Temporary beam tendons	ϕ15.2 mm × 12 strands per duct $f_{pi} = 0.8 f_{py} = 1{,}255.3$ MPa
	Continuity tendons	ϕ15.2 mm × 12 strands per duct $f_{pi} = 0.8 f_{py} = 1{,}255.3$ MPa
	μ, k	$m = 0.25$/rad, $k = 0.0050$/m, relaxation = 5%

assumed that the bridge width for all spans was 12.5 m to accommodate three traffic lanes and five U-shaped girders spaced 2.5 m center-to-center as shown in Fig. 4(a). Sectional design was completed only for the G1 girder because the exterior member in this type of bridge usually experiences the critical demand. Fig. 4(b) depicts a representative longitudinal section of one span with the constant dimensions and range of variable dimensions corresponding to the range of span lengths considered (25-45 m). Fig. 5 shows the tendon arrangement for a left span with a length of 40 m. The overall layout is approximately the same for the other span lengths, but the detailed tendon profile depends on the selected cross-sectional dimensions. Table 1 lists the assumed material properties for the concrete and tendons.

3.2 Sectional database

A sectional database was generated from the basic geometry of the U-shaped precast girder and the cast-in-place deck slab shown Fig. 6. From this database, an optimal section was determined for each example span length. Basic database geometry was based on the U-shaped section of an actual prestressed concrete bridge with the span length of 30 m (Korea Highway Corporation 1997). To simplify the generation of candidate sections, some dimensions were held constant (slab thickness,

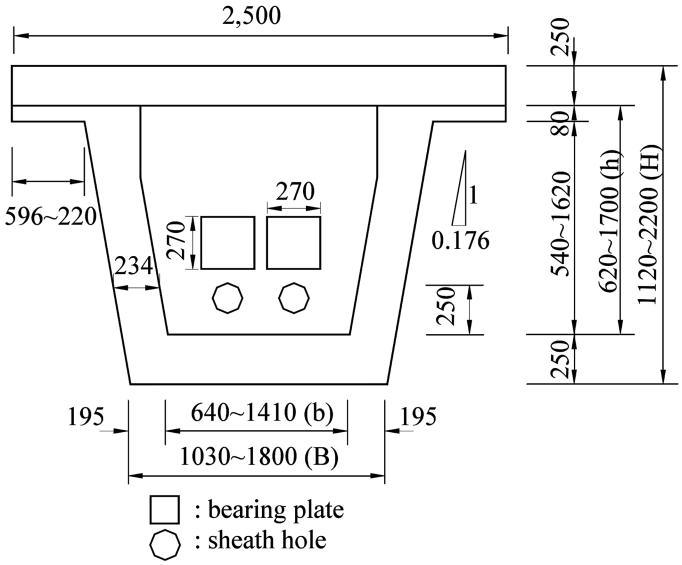

Fig. 6 Basic geometry of U-shaped girder including slab (unit: mm)

top and bottom flange thickness, web thickness, and slope of web). The ranges of variable dimensions are indicated in Fig. 6.

The geometry of the U-section controlled the possible configurations of tendon ducts. The section dimensions had to be large enough to accommodate the minimum bearing plate dimensions and prestressing jack clearance requirements (VSL 1998). The assumed size and number of strands in each type of tendon are listed in Table 1.

The minimum internal width (b) of the bottom flange included in the database was 640 mm. This would permit installation of two 270-mm-square bearing plates in a row with a clear spacing of 100 mm. The minimum internal depth (h) of 620 mm also was determined by considering the bearing plate dimensions and jack working clearance requirements. On the other hand, the 220-mm minimum width of the top flange overhang resulted from an investigation by Ralls *et al*. (1993).

Based on the aforementioned conditions, a database of 77 sections was obtained by increasing the bottom flange width and girder depth by 100-mm increments in each direction until the maximum dimensions shown in Fig. 6 were reached. The maximum total depth (including slab) of the sections was limited to 2.2 m based on a typical bridge depth of 2 m.

3.3 Structural analysis and selection of optimum sections

A number of structural analyses were performed for each span. All sections in the database were investigated in turn. The RM-SPACEFRAME computer program (Pircher 1996), which has the capacity to consider time-dependent behavior of prestressed concrete members, was used in this study. Creep and shrinkage were modeled according to CEB-FIP recommendations (CEB-FIP 1990). The construction procedure was numerically modeled using nine analysis stages. Fig. 7 describes the nine stages for the model of a 40-m span bridge. The labels such as 1 through 72 for the girders as well as 201 through 272 for the slab indicate the element numbers for the frame

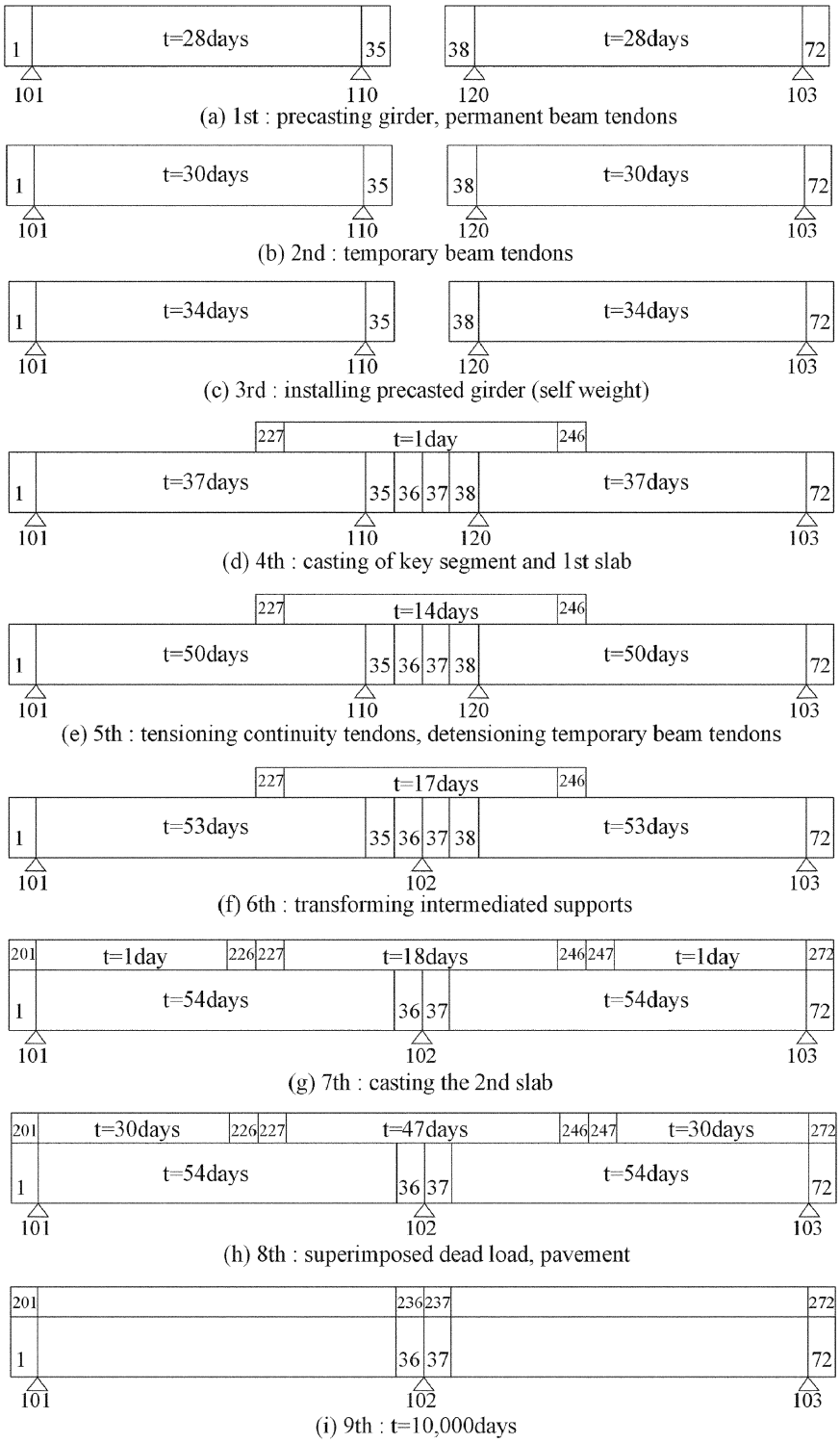

Fig. 7 Analysis stages to simulate the proposed method

analysis. The labels such as 101, 103, 110, and 120 represent support nodes. Labels such as t = 1 day indicate the assumed concrete age at the stage under consideration. The time of each stage was assumed according to experience with construction of similar actual bridges.

After the structural analysis considering each construction stage was completed, the traffic loads and superimposed dead loads, including pavement, were applied to the model of the completed two-span continuous bridge. Traffic loads were taken as the Korean DB24 truck loading and equivalent lane loading (DL24) (KSCE 1996). Additionally, the effects of temperature differential and support settlement were also considered. The temperature difference between the slab and precast girder was taken as $\pm 5^{o}$C and the support settlement was taken as ± 10 mm.

After the structural analysis, the service and strength limit states for the analyzed sections were checked in accordance with the Korean Highway Bridge Design Specification (KSCE 1996). Because this is a fundamental study, the preliminary design checks were limited to flexural behavior. It can be assumed that the designs were conservative enough to satisfy concerns about other design conditions such as shear strength.

In order to select the optimal section for each span from a database of 77 sections, the structural efficiency was also considered using Guyon's (1953) sectional efficiency factor (ρ):

$$\rho = \frac{r^2}{y_b y_t} \tag{1}$$

r = radius of gyration of the section $\frac{A}{I}$

y_b = distance from the centroid to the bottom fiber of the section

y_t = distance from the centroid to the top fiber of the section

Inspection of the sectional efficiency factors for all database sections revealed that the highest efficiencies correspond to sections with the smallest bottom-flange widths and smallest depths. Therefore, the optimal section for each span length was selected as the one with the smallest width and depth among those sections satisfying strength and serviceability requirements.

3.4 Comparison of design results to existing practice

Table 2 lists the optimal database sections for each span length. Fig. 8 represents a comparison of the optimal sections to standard simply supported, precast I-girder designs (Korea Highway

Table 2 Design results

Span (m)	B (cm)	H (cm)	Permanent beam tendons	Temporary beam tendons	Continuity tendons
25	130	135	2R 2C	1R 3C	1R 3C
30	130	145	2R 2C	1R 3C	1R 2C+1R 3C
35	130	175	3R 2C	1R 3C	1R 3C+1R 3C
40	130	205	3R 2C	1R 2C+1R 3C	2R 3C
45	130	220	3R 2C	1R 2C+1R 3C	1R 2C+2R 3C

nR : n tendon holes in a row (layer)
nC : n tendon holes in a column

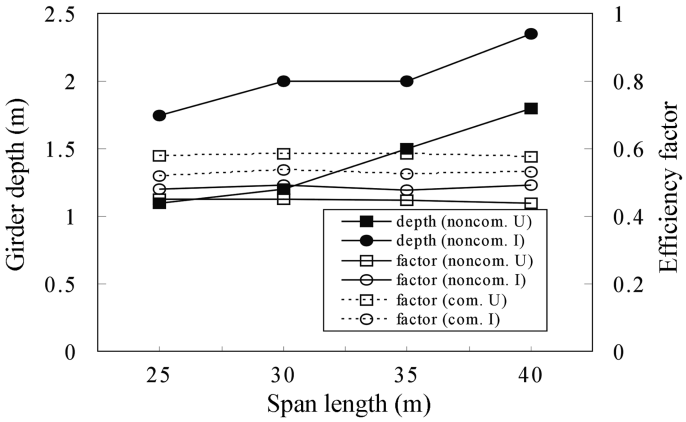

Fig. 8 Comparisons of girder depths and sectional efficiency factors

Corporation 1996). The lines with solid markers indicate the girder depth; the lines with open markers indicate Guyon's sectional efficiency factor. For each section, the noncomposite and composite (including slab) efficiency factors are plotted. The plotted girder depth corresponds to the depth of the precast section only.

In the case of the I-shaped precast girder, the depths range from 1.75 m for a 25-m span to 2.35 m for a 40-m span length. However, the optimal spliced U-girder depths range from 1.10 m for a 25-m span to 1.95 m for a 45-m span. Over the investigated span range, the girder depths are reduced by approximately 500-800 mm. For the 30-m span–one of the most common spans for the I-shaped section–the depth reduction is about 800 mm (36 percent of the composite I-girder depth). For the 40-m span, the depth of the composite girder decreases from 2.60 m to 2.05 m. In spite of this 21 percent reduction in depth, the live load deflection limit (span length/1000) is not exceeded.

Fig. 8 indicates that Guyon's sectional efficiency factors are fairly constant over the range of span lengths investigated. Considering noncomposite sections, the I-girders exhibit slightly higher efficiency factors (~0.49) than the U-girders (~0.45). On the other hand, the composite U-girders exhibit slightly higher factors (~0.58) than the composite I-girders (~0.53). Although the structural efficiency factors are comparable, the significant depth reduction resulting from the proposed method results in a lighter superstructure, reduced earthwork, and a more slender appearance. Thus, application of the proposed splicing technique with a U-shaped girder can be more efficient than utilization of simply supported I-shaped girders.

4. Flexural behavior during splicing operations

4.1 Sequence of tensioning and detensioning operations

For the proposed method, the tensioning and detensioning processes are essential for inducing the secondary moment during the splicing stage, which is shown in Fig. 1(e). The structural analyses described previously are based on the assumption that tensioning of continuity tendons and detensioning of temporary beam tendons occur simultaneously. This is unrealistic because some amount of time must elapse between the two operations. In one scenario, all the temporary beam

tendons are detensioned after prestressing of the continuity tendons. In the opposite scenario, detensioning is performed prior to prestressing of the continuity tendons.

For the first scenario, tension stresses will exceed allowable levels at the bottom of sections over the continuous support immediately after prestressing of the continuity tendons. The induced secondary (negative) moment is not yet large enough to generate the necessary compressive stresses in the bottom fiber because the temporary beam tendons have not been detensioned. For the second scenario, much of the concrete near the continuous support would be stressed to excessive levels immediately after completion of detensioning operations. The lack of effective tendons in this region during this period results in an obviously unsafe design. Completion of either the tensioning or the detensioning process prior to initiation of the other causes undesirable stress conditions. Therefore, the tensioning and detensioning operations should be alternated until the desired stress levels are reached.

4.2 Sensitivity of tensioning and detensioning operations

This section addresses which operation–tensioning of continuity tendons or detensioning of temporary tendons–should be performed first, and to what degree the first operation should be completed prior to initiation of the second. A bridge with a 40-m span serves as an example. The structural model, analysis procedure, material properties, geometry, and tendon layout are consistent with the procedures and values described in Section 3. Fig. 9 shows typical sectional geometry of the example girder.

Fig. 10 depicts bending stresses in the left span immediately after prestressing of the continuity tendons and prior to detensioning of temporary tendons (Fig. 11). Tensile stresses are labeled as positive. Fig. 10(a), (b), and (c) illustrate stresses at the top and bottom fibers of the precast U-section and the top fiber of the cast-in-place slab, respectively. Each line represents application of a

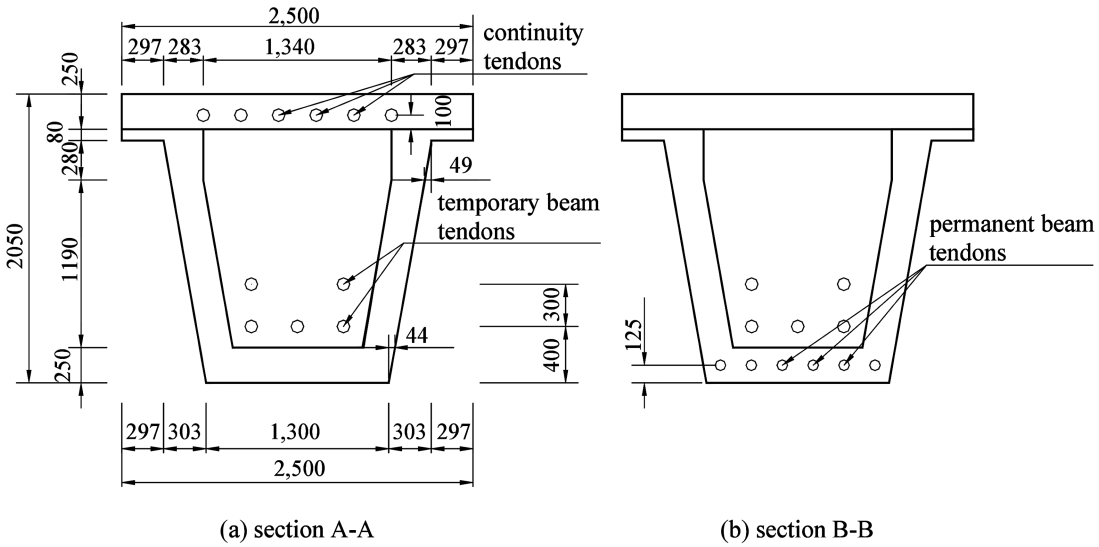

Fig. 9 Typical girder sections in 40-m span (see to Fig. 4, unit: mm)

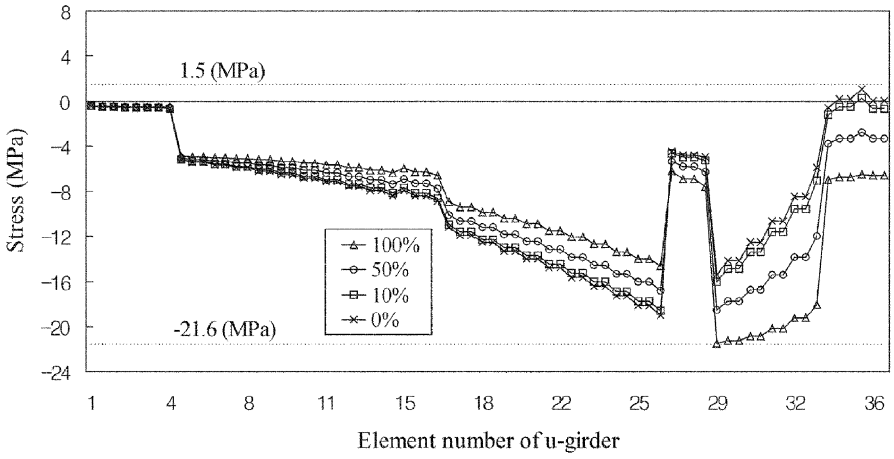

(a) Top fiber of U-shaped girder

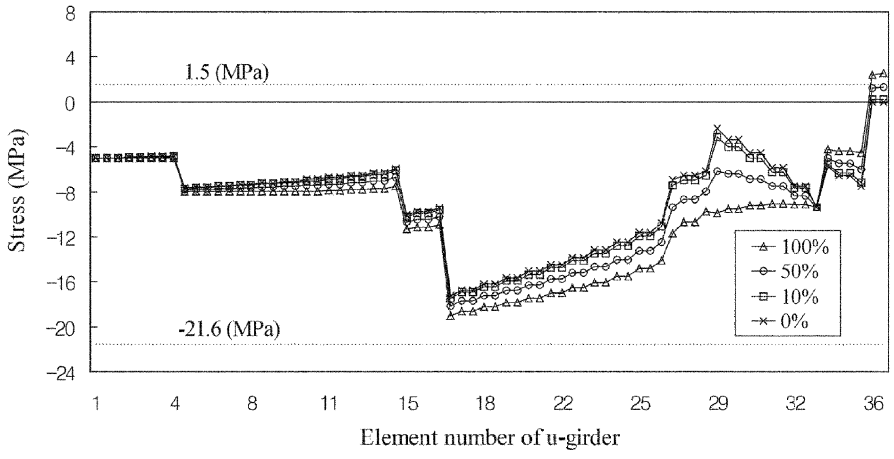

(b) Bottom fiber of U-shaped girder

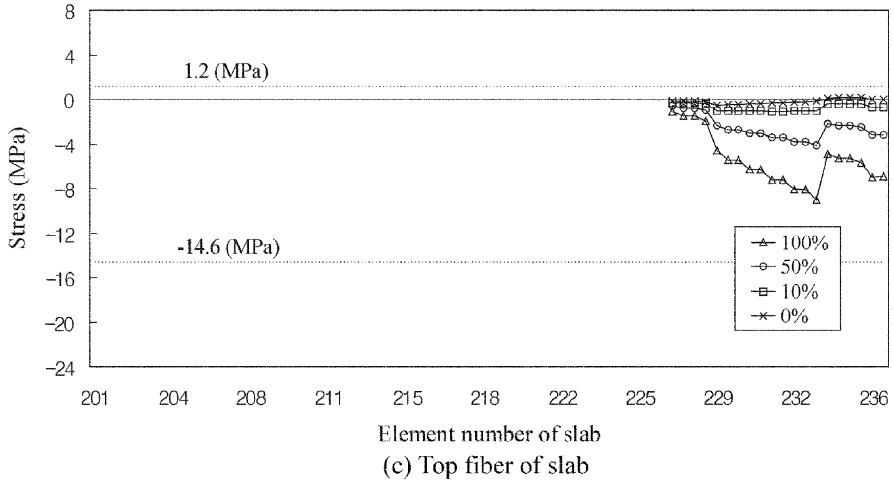

(c) Top fiber of slab

Fig. 10 Bending stress after tensioning continuity tendons

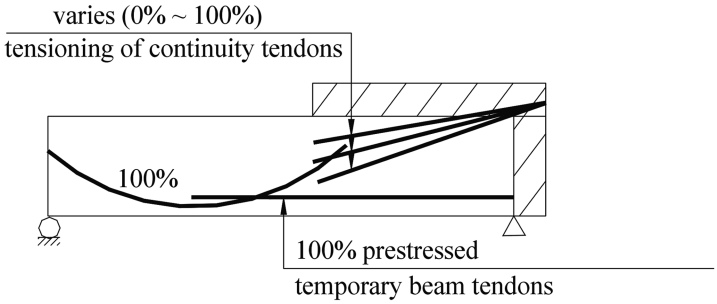

Fig. 11 Conceptual diagram for the procedure of prestressing operations in Fig. 10

particular portion (0%, 10%, 50%, 100%) of the total design prestress for the continuity tendons. For example, "50%" represents the case when all of the continuity tendons are tensioned to half of the design initial prestressing force for these tendons.

The stresses at the top fibers of the girder and slab are within the range of allowable stresses for any portion of total prestressing applied. However, the bottom fiber stress exceeds the allowable tensile stress when large portions of the continuity prestressing are applied prior to detensioning of temporary tendons. From these results, the upper bound for the tensioning force that could be applied first was computed to be 58.2 percent of the total design prestress force.

Stresses are shown in Fig. 12 for the case when a portion of the detensioning operation is performed prior to prestressing of continuity tendons (Fig. 13). Each line represents the stresses immediately after detensioning a particular portion (0%, 10%, 50%, 100%) of the total prestressing force in the temporary tendons.

Comparison of Fig. 10 and Fig. 12 indicates that the sequence that begins with partial detensioning (Fig. 12) is more sensitive than the sequence that begins with partial prestressing of the continuity tendons (Fig. 10). Only a 17.7 percent reduction of the total prestressing force in the temporary tendons can be achieved prior to exceeding allowable stress limits. Thus, a sequence characterized by partial prestressing of the continuity tendons prior to detensioning of the temporary beam tendons is likely to require fewer stressing operations than a sequence that begins with partial detensioning of the temporary tendons.

4.3 Optimum amount of tensioning and detensioning in each step

From an economic point of view, the number of jacking operations should be minimized. Thus, it is desirable that complete detensioning of the temporary tendons be performed in a single step after the initial partial prestressing of the continuity tendons.

Fig. 14 depicts stresses after a portion of continuity tension is applied and then complete detensioning of the temporary tendons is performed (Fig. 15). Each line represents the portion of the design tensioning force applied to the continuity tendons prior to detensioning of the temporary tendons. At least 51.9 percent of the total continuity prestressing force must be applied in the first step so that allowable stresses are not exceeded after the second step of complete detensioning of temporary tendons. As may be seen in Fig. 14(b), this value is required to prevent excessive tensile stresses in the bottom fiber of the U-section.

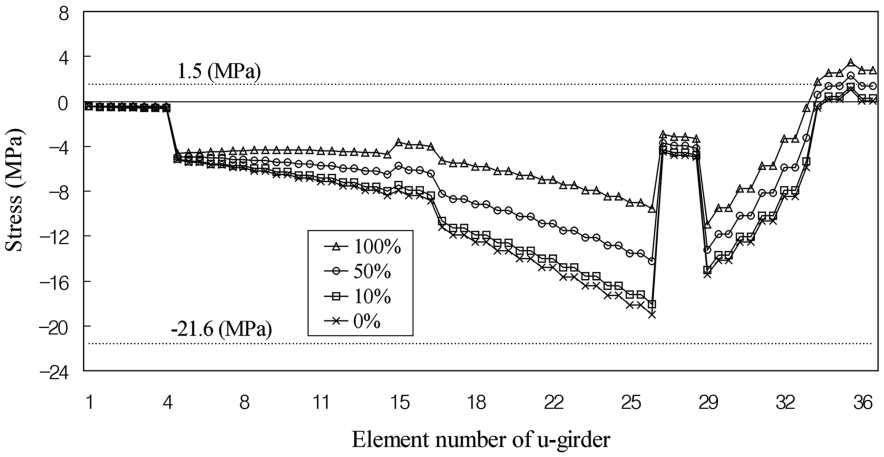

(a) Top fiber of U-shaped girder

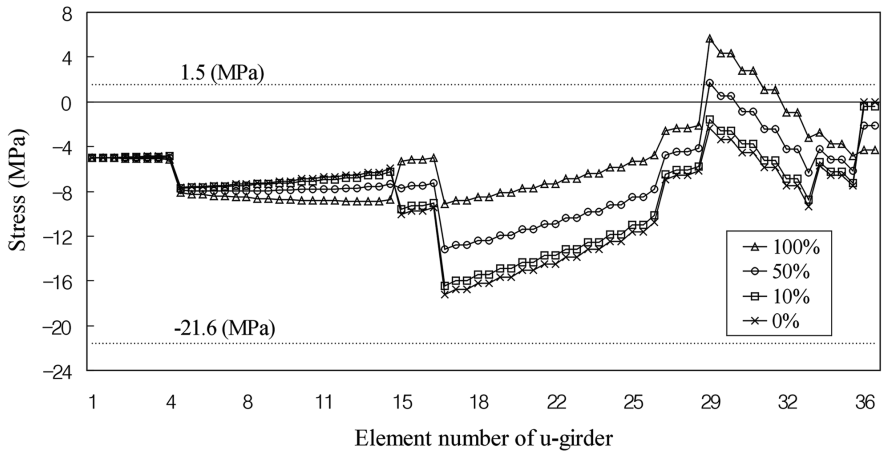

(b) Bottom fiber of U-shaped girder

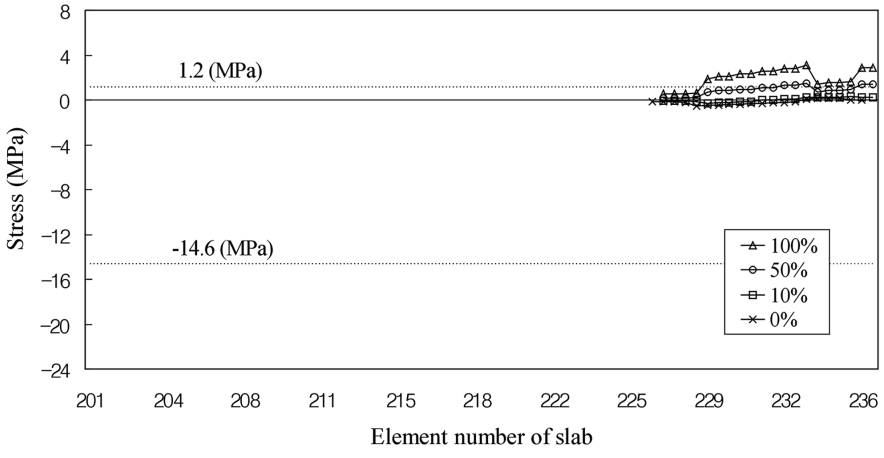

(c) Top fiber of slab

Fig. 12 Bending stress after detensioning temporary tendons

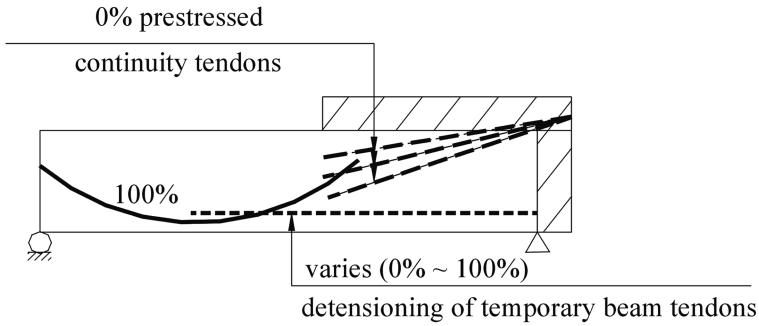

Fig. 13 Conceptual diagram for the procedure of prestressing operations in Fig. 12

To satisfy allowable stress requirements in all construction stages, the initial tensioning rate of the continuity tendons must be between this lower-bound value of 51.9 percent and the upper-bound value of 58.2 percent obtained from the analysis described Section 4.2. Thus, the splicing sequence for this example bridge was divided into three steps. The initial tensioning rate applied to the continuity tendons was 55 percent. Then the temporary beam tendons were completely detensioned. The splicing sequence concluded with application of the remaining 45 percent of the continuity prestressing force.

Fig. 16 shows the stresses just after all three steps of the splicing sequence. Fig. 17, Fig. 18, and Fig. 19 depict stresses immediately after completion of construction as well as the stresses resulting from critical service loads. These figures show that the stresses in the precast and cast-in-place sections are within allowable limits at all stages.

The maximum factored moment and design flexural strength, the cracking moment, and the maximum traffic load deflection of the girder are listed in Table 3. All of these performance characteristics were satisfactory.

4.4 Practical simplification of splicing sequence

In practice, it may be excessively difficult to compute the optimal amounts of sequential tensioning and detensioning for the three-step splicing sequence proposed. Therefore, it may be better to reduce the steps as much as possible.

In the example bridge, exceeding the upper-bound limitation on initial prestressing of the continuity tendons causes excessive stresses only in the bottom fibers of the cast-in-place concrete sections over the continuous support (Fig. 10(b)). However, these temporarily over-tensioned fibers are soon compressed when the temporary beam tendons are detensioned.

Thus, if the bottom of the cast-in-place joint is appropriately reinforced, the splicing sequence can be simplified to a two-step process of full continuity prestressing followed by complete detensioning of temporary tendons. Fig. 20 shows the stresses in the example bridge after completion of this two-step splicing sequence. Because of the relatively short time required for the splicing sequence, time-dependent effects are inconsequential. Therefore, stresses shown in Fig. 20 are practically indistinguishable from those in Fig. 16.

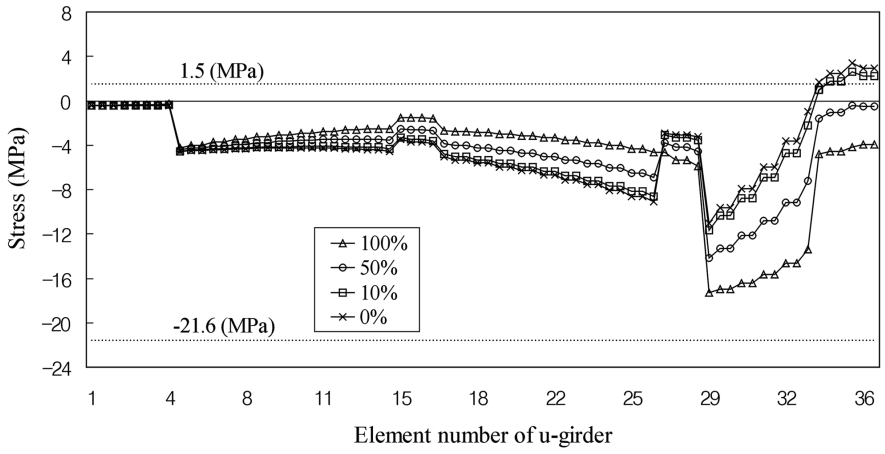

(a) Top fiber of U-shaped girder

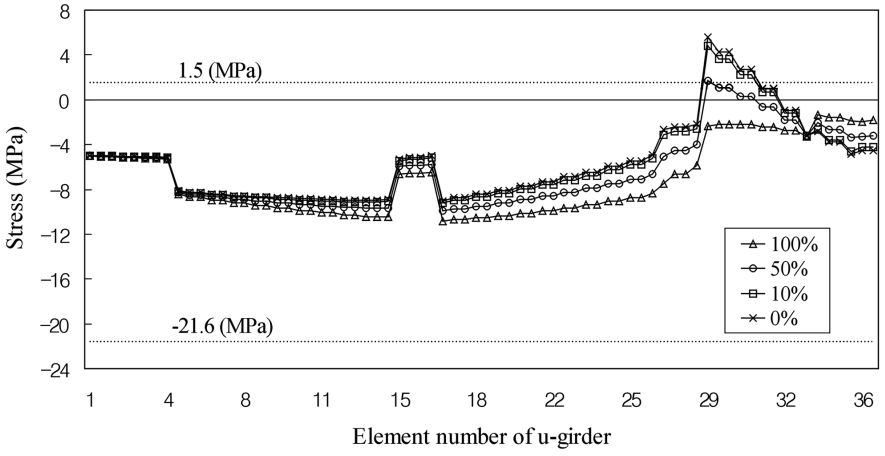

(b) Bottom fiber of U-shaped girder

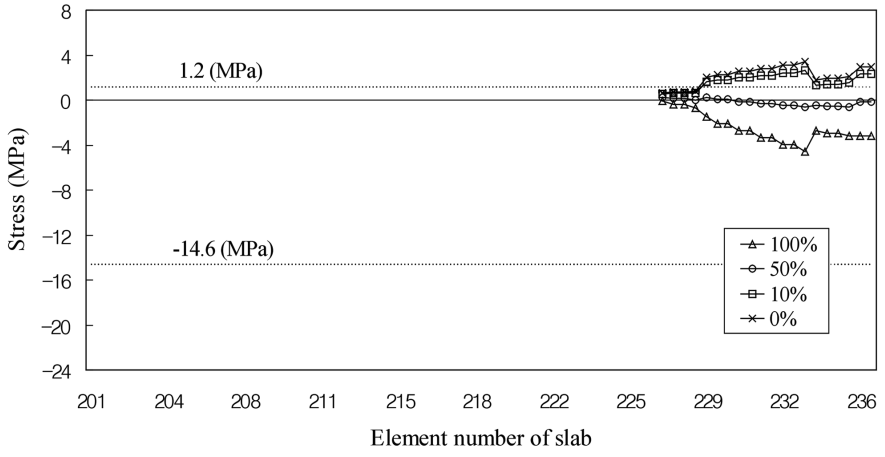

(c) Top fiber of slab

Fig. 14 Bending stress after complete detensioning dependent on amount of initial continuity prestressing

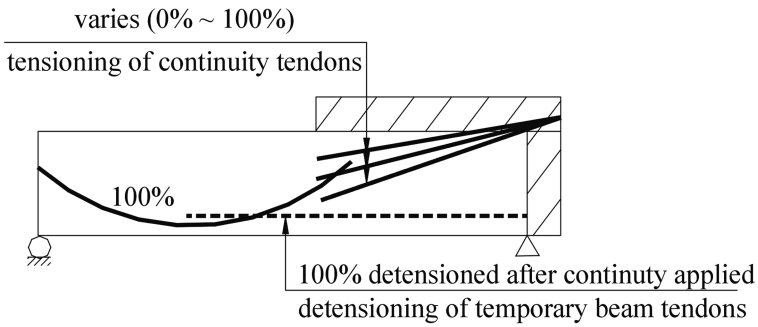

Fig. 15 Conceptual diagram for the procedure of prestressing operations in Fig. 14

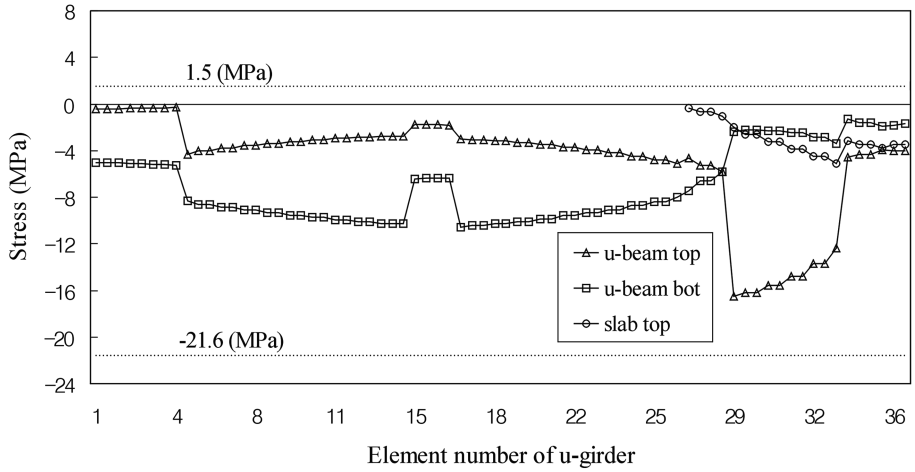

Fig. 16 Bending stress after the splicing stage

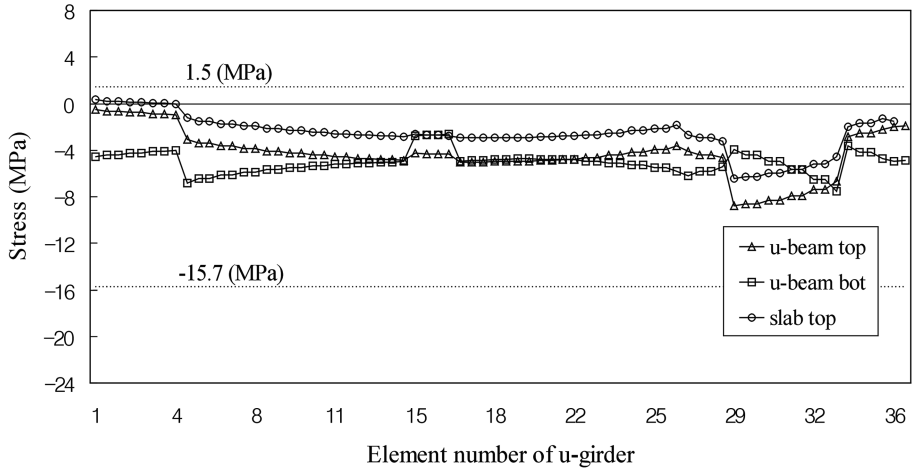

Fig. 17 Bending stress at completion of construction

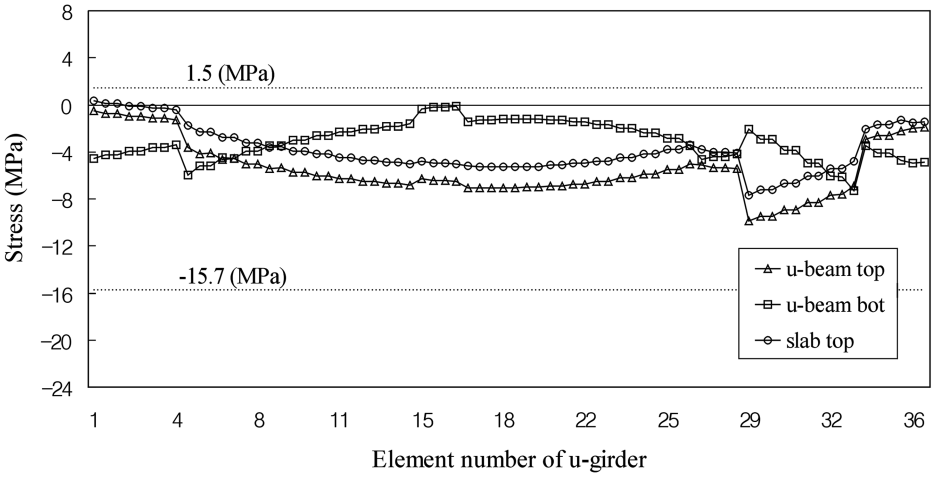

Fig. 18 Bending stress under critical service loads for positive moment

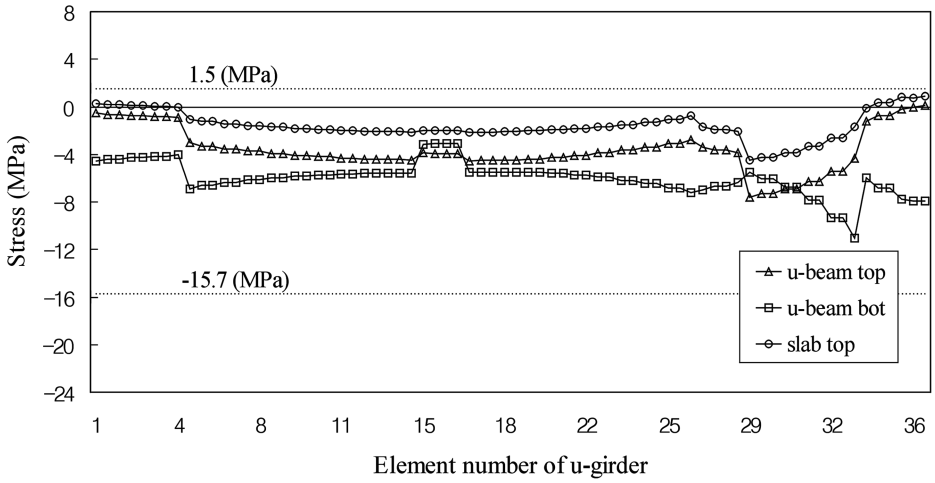

Fig. 19 Bending stress under critical service loads for negative moment

Table 3 Performance characteristics of example bridge

Section	M_u^* (kN · m)	ϕM_n^* (kN · m)	M_{cr} (kN · m)	$\frac{\phi M_n}{M_{cr}}$	Δ (mm)	Δ_{limit} (mm)
Midspan	17,140	21,580	14,360	1.50	15.4	40
Continuity support	13,520	26,130	13,290	1.97	-	-

*load combination : 1.3D+2.15L, strength reduction factor ϕ: 0.85

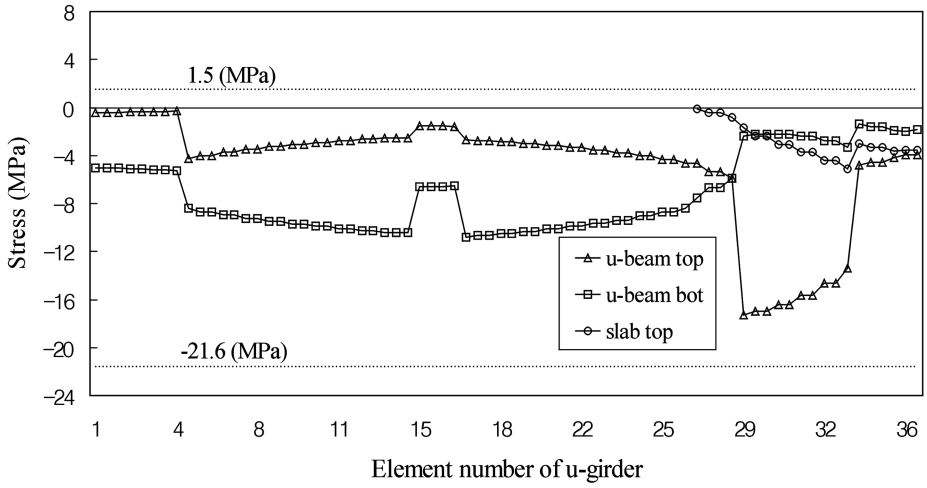

Fig. 20 Bending stress after the splicing stage when the continuity tendons are completely tensioned first

5. Conclusions

A new technique for splicing two precast spans to form a continuous bridge has been introduced. The method is unique because it intentionally induces a secondary moment to improve the efficiency of the continuous structure. This secondary moment transforms the self-weight bending moment diagram into a shape similar to that characteristic of a continuous bridge.

Use of the proposed splicing method with U-shaped candidate sections resulted in beam depth reductions of 500-800 mm for moderate-span bridges compared to standard precast I-girders.

During the splicing procedure, partial or complete prestressing of continuity tendons must precede detensioning of the temporary tendons. Establishing the required minimum amount of continuity prestressing prior to detensioning requires careful consideration.

A numerical investigation of the flexural behavior of a spliced bridge with 40-m spans indicates that the stresses in the sections develop as intended through the various construction and service stages.

References

Abdel-Karim, A.M. and Tadros, M.K. (1992), *State-of-the-Art of Precast/Prestressed Concrete Spliced-Girder Bridges*, Prestressed/Prestressed Concrete Institute (PCI), Chicago.

CEB-FIP (1990), *Model Code for Concrete Structures: CEB-FIP International Recommendations*, Comite Euro-International du Beton, Paris.

Girgis, A., Sun, C. and Tadros, M.K. (2002), "Flexural strength of continuous bridge girders-Avoiding the penalty in the AASHTO LRFD specifications", *Open Forum: Problems and Solutions, PCI Journal*, **47**(4), 138-141.

Guyon, Y. (1953), *Prestressed Concrete*, John Wiley & Sons, New York.

Korea Highway Corporation (1996), *Typical Drawings for Highway Construction.*

Korea Highway Corporation (1997), *Drawings for DaeYa Bridge*.

KSCE (1996), *Highway Bridge Design Specifications*, Korea Ministry of Construction and Transportation.
Lee, H.W., Kim, M.S. and Lee, Y.D. (2000), "Structural behaviour of the continuous bridge of two spans spliced by using the secondary moment", *Proc. European Congress on Computational Methods in Applied Sciences and Engineering (ECCOMAS 2000)*, 1-11.
Pircher, H. (1996), *RM-SPACEFRAME rev.5.70*, TDV, Graz, Austria.
Ralls, M.L., Ybanez, L. and Panak, J.J. (1993), "The new Texas U-beam bridges: an aesthetic and economical design solution", *PCI Journal*, **38**(5), 20-29.
Ronald, H.D. (2001), "Design and construction considerations for continuous post-tensioned bulb-tee girder bridges", *PCI Journal*, **46**(3), 44-66.
Russell, B.W. (1994), "Impact of high strength concrete on the design and construction of pretensioned girder bridges", *PCI Journal*, **39**(4), 76-89.
Tadros, M.K., Ficenec, J.A., Einea, A. and Holdsworth, S. (1993), "A new technique to create continuity in prestressed concrete members", *PCI Journal*, **38**(5), 30-37.
VSL (1998), *Post-Tensioning System*, VSL International LTD., Berne, Switzerland.
Weigel, J.A., Seguirant, S.J., Brice, R. and Khaleghi, B. (2003), "High performance precast, pretensioned concrete girder bridges in Washington state", *PCI Journal*, **48**(2), 28-52.